Int. J. Multiphase Flow Vol. 7, pp. 47–61
Pergamon/Elsevier, 1981. Printed in Great Britain

0301-9322/81/0201-0047/$02.00/0

AN EXPERIMENTAL STUDY OF THE EFFECT OF THE AXIAL HEAT FLUX DISTRIBUTION ON THE DRYOUT CONDITIONS IN A 3650-mm LONG ANNULUS

KURT M. BECKER and ADAM LETZTER
The Royal Institute of Technology, Stockholm, Sweden

and

OLOV NYLUND and BERTIL SCHÖLIN
ASEA-ATOM, Västerås, Sweden

(*Received* 25 *September* 1979; *in revised form* 28 *July* 1980)

Abstract—Dryout measurements have been carried out for flow of boiling water in a 3650-mm long annulus. Eight different axial heat flux profiles, typical for BWRs, as well as one with uniform heat flux have been studied. It was found that for the present geometry the effect of the axial heat flux profile upon the total dryout power was rather small or in the range of ±6 per cent.

1. INTRODUCTION

The basis for dryout predictions in boiling water reactors is full scale rod bundle experiments. However, since such tests are expensive, and available analytical methods still need a strong empirical support, the influence of various parameters has to be established as far as possible by simpler experiments. For two reasons, this is very desirable in the case of the axial heat flux distribution. First, there are large variations in the axial heat flux distribution for BWR fuel assemblies as a function of both core position and time. However, at present those variations are being reduced considerably by an advanced use of burnable absorbers. Secondly, a new set of heater rods is needed each time a new axial heat flux distribution is to be investigated in a dryout experiment, which makes such variations very expensive in the case of full scale 8 × 8-bundles.

Systematic investigations of the influence of the axial heat flux distribution on dryout are relatively few in the open literature, even for simple geometries. Among the studies, which cover conditions relevant to BWRs, may be mentioned round tube data by Judd *et al.* (1967) and Becker *et al.* (1969), annular data by Judd *et al.* (1967), Janssen & Kervinen (1963) and Little (1970), and rod bundle data by General Electric (1973) and Lee & Bailey (1977). An interesting analytical contribution is given in a recent paper by Lahey & Gonzalez-Santalo (1977), where a unique relation between the *F*-factor method by Tong (1972) and the critical quality-boiling length method is demonstrated, and a relation between uniform and non-uniform axial distribution data is derived.

The present investigation was carried out a few years ago to supplement the existing ASEA-ATOM dryout data base, ranging from 4- to 64-rod bundles. It was performed in full length annular geometry and included nine different axial heat flux distributions. Although the results of an annulus are not directly applicable to full scale rod bundles we feel that these data may represent a signifiacant contribution on the way to a full understanding of the influence of axial heat flux distribution on dryout.

2. APPARATUS AND TEST SECTION

The measurements were carried out employing the 1-MW loop at the Royal Institute of Technology. This loop was designed for an operating pressure of 250 bar, and all parts of the loop in contact with water were made from stainless steel. A simplified flow diagram for the loop is shown in figure 1. Test sections with heated length up to 7200 mm can be studied, and the power is supplied from a direct current generator. The maximum available current is 6000 A and voltages ranging from 0 to 140 V can be supplied.

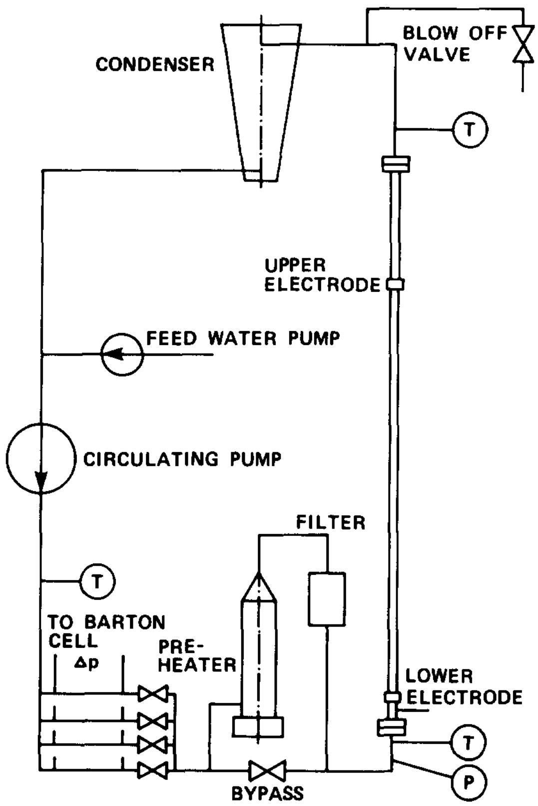

Figure. 1. Flow diagram.

Before entering the test section the water passes a 150-kW preheater and a filter. The preheater was used for adjusting the inlet water temperature. After the test section the steamwater mixture flows through a condenser, and the water then enters the circulation pump, which has a pressure head of 100 m of water. The major portion of this pressure head was used in the duct system between the pump and the test section inlet, thus providing sufficient throttling for securing stable operation of the loop.

2.1 *Test section*

The annular test section consisted of two concentric stainless steel tubes. The inner and the outer diameters of the annulus were 12.25 and 20.43 mm, giving an annulus gap of 4.09 mm. The heated length of the inner tube was 3650 mm. It should be noticed that the rod diameter and the heated length were chosen to represent the ASEA-ATOM BWR fuel element geometry.

The inner cylinder was kept in its central position by means of seven sets of spacers, which were mounted on the outer cylinder. The distance between the spacers was 510 mm, and each set of spacers consisted of three 2-mm stainless steel pins, 120° apart. The pins were adjusted by means of micrometers, and were insulated from the outer tube by means of Teflon gaskets. This spacer design had negligible effects on the flow conditions in the annulus.

In order to obtain the desired axial heat flux profiles, the wall thickness of the inner electrically heated tube was varied axially, keeping, however, the outer diameter of the heated tube constant.

At the exit the inner rod was extended with a 150-mm long unheated section. This was achieved by soldering a copper rod to the inside wall of the inner tube.

The water was supplied to the test section through two 20-mm i.d. ducts 180° apart. A similar arrangement was also provided for the exit steam-water mixture.

As mentioned earlier, the objective of the present study was to test eight rods with different axial heat flux profiles and one rod with uniform heat flux. After the heater tubes had been received from the manufacturer, the axial variations of the electrical resistance were measured, and it was found that along the full length, the profiles differed less than 3 per cent from the desired values. Figures 2 and 3 show the relative power vs length for the eight non-uniform rods.

2.2 *Dryout detection*

In order to protect the test section from destruction, dryout detectors were used to switch off the power supply when excessive temperature excursions occured on the heated rod. Since it may be possible for dryout to occur at any position downstream of the heat flux peak, the full length of the heated rod downstream of the peak had to be protected. To be able to determine the approximate dryout position, 6 dryout detectors of the Wheatstone bridge type were employed. Three of the detectors used the 2-mm dia. spacer pins as electrodes. However, the 510-mm distance between the spacers was considered too large for a satisfactory determination of the dryout location. Therefore three additional dryout detectors were attached to the heated rod by welding the leads to the inner wall. The leads were taken to the exterior through a hole in the copper bar at the upstream end of the heated tube. Figures 4 and 5 show the locations of the dryout detectors for the eight non-uniformly heated rods.

3. METHOD OF TESTING AND RANGES OF VARIABLES

During the course of a particular run the pressure, the mass velocity and the inlet water temperature were kept constant at prescribed values, while the power supplied to the test section, was gradually increased by small steps until dryout occurred. Just before dryout these steps amounted to less than 1 per cent of the power, and one set of data was taken after each increase by means of a Schlumberger data collecting system. The last set of data obtained before the dryout detectors reacted, was used to evaluate the dryout conditions.

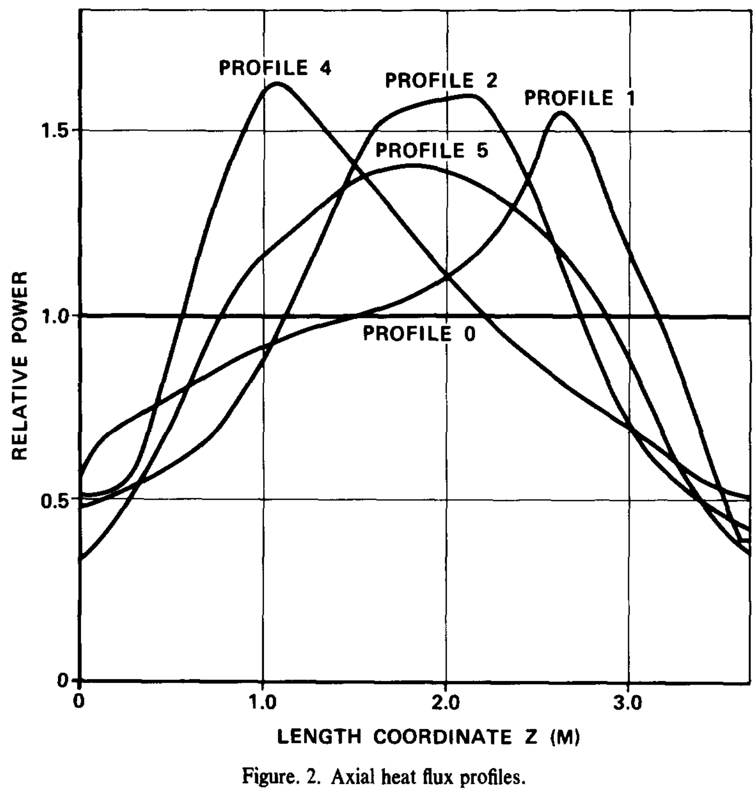

Figure. 2. Axial heat flux profiles.

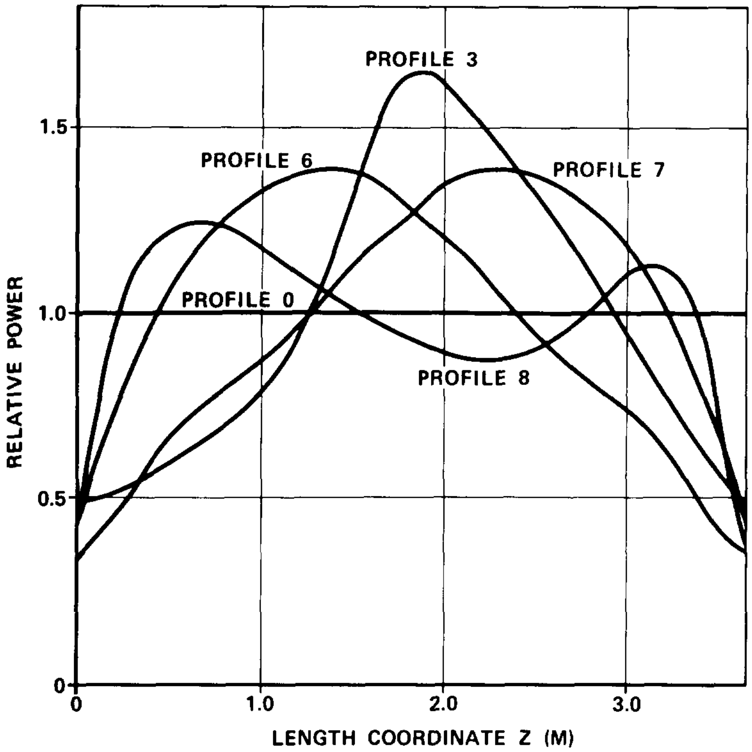

Figure. 3. Axial heat flux profiles.

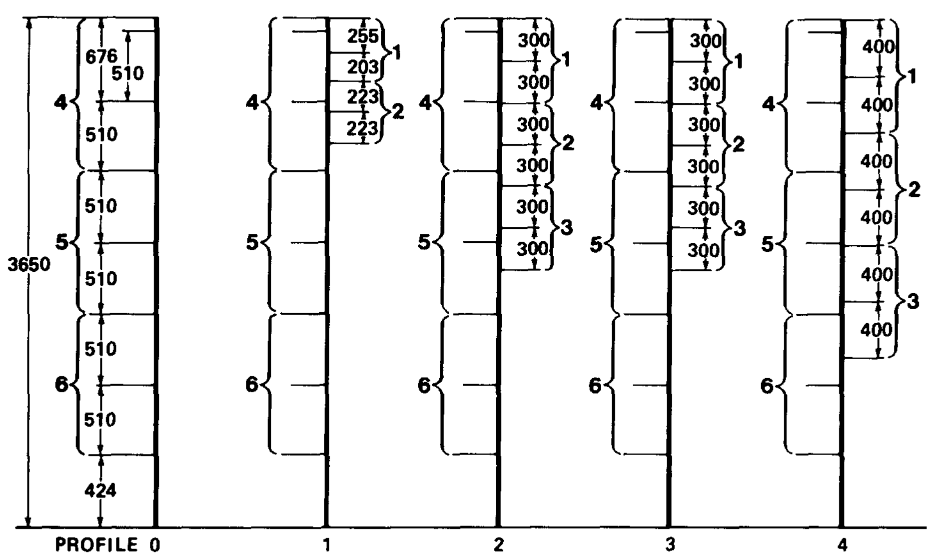

Figure 4. Locations of dryout detectors.

In all, 221 runs were obtained at the following conditions:

Heated length	L = 3650 mm
Inner diameter (i.d.)	d_i = 12.25 mm
Outer diameter (o.d.)	d_o = 20.43 mm
Pressure	p = 70 bar
Inlet sub-cooling	Δt_s = 10 and 40°C.

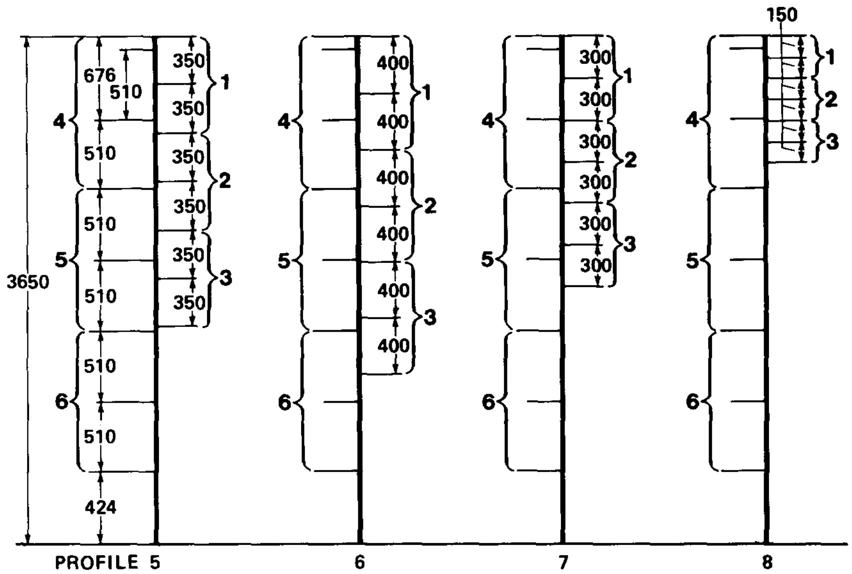

Figure 5. Locations of dryout detectors.

With regard to the mass velocity the following values were originally selected

$$G = 250, 500, 750, 1000, 1250, 1500, 2000 \text{ and } 2500\,\text{kg/m}^2\text{s}.$$

In order to verify the reproducibility of the measurements, the experiment started with the low mass velocity and 10°C sub-cooling. After this test series was finished, the 40°C sub-cooling tests were carried out, and finally 10°C sub-cooling measurements were obtained starting at the highest mass velocity and taking data at the following mass velocities.

$$G = 375, 625, 875, 1125, 1375, 1750 \text{ and } 2250\,\text{kg/m}^2\text{s}.$$

It was found that the two series of 10°C sub-cooling tests were in perfect agreement with one another, proving the reproducibility of the measurements.

Since the investigation, which covered nine test sections, lasted for more than 3 months, the reproducibility of the equuipment was also checked by running the uniform heat flux test section at two occasions. The research program started with this test section, and after running the eight axial profiles, the uniform test section was again employed to complete the investigation. In the figures the uniform heat flux measurements are referred to as profile 0, and in table 1 the labels 0 and 9 are used for the initial and the final uniform heat flux measurements. The dryout powers measured at the two occasions differed less than 1 per cent. Hence one may conclude that during the whole investigation the apparatus yielded reproducible dryout results.

4. EXPERIMENTAL RESULTS AND DISCUSSIONS

The experimental results are given in table 1, and in figures 6–13 the data are reproduced in plots of the total dryout power, Q, vs the mass velocity, G. The total dryout power was chosen as the most representative parameter because of the difficulty of determining the exact heat flux at the dryout position. This difficulty was introduced by the dryout detection system, which generally gave the dryout location with a resolution of about 100–200 mm. It should be noticed, however, that for the test section with uniform heat flux dryout always occured at the exit. Also for the test sections 3, 4, 5, 6, 7 and 8 dryout probably occurred at the exit, except for a few runs for test sections 5 and 6 at $G > 2000\,\text{kg/m}^2\text{s}$. Exit dryout is indicated by the fact that only the downstream dryout detector reacted, demonstrating the presence of dryout in the down-

Table 1.

Run no	p bar	Δt_{in} ^oC	G kg/m^2s	Q kW	x_{ex}	z_{BO} mm	x_{BO}
Profile No. 0 (Uniform)							
101	69.85	11.32	250.4	46.6	0.5476	3600.	0.5395
102	69.56	10.05	385.9	64.1	0.4884	3600.	0.4813
103	70.05	10.05	507.5	78.5	0.4539	3600.	0.4472
104	69.36	9.62	623.9	91.1	0.4268	3600.	0.4205
105	69.85	9.86	751.7	103.6	0.4007	3600.	0.3948
106	69.76	9.76	866.1	111.4	0.3717	3600.	0.3661
107	69.46	8.98	1014.	123.1	0.3512	3600.	0.3459
108	69.76	9.76	1137.	128.9	0.3237	3600.	0.3188
109	70.05	10.78	1258.	136.0	0.3041	3600.	0.2994
110	69.76	10.00	1377.	141.0	0.2883	3600.	0.2838
111	69.26	10.01	1505.	147.4	0.2736	3600.	0.2694
112	69.66	10.15	1753.	154.5	0.2426	3600.	0.2387
113	70.15	10.63	2006.	165.4	0.2235	3600.	0.2200
114	69.66	9.91	2234.	169.9	0.2054	3600.	0.2021
115	70.05	9.81	2478.	178.3	0.1929	3600.	0.1898
401	69.66	39.75	249.9	52.1	0.5247	3600.	0.5157
402	70.05	40.14	501.3	90.6	0.4370	3600.	0.4292
403	69.76	40.09	750.4	121.8	0.3784	3600.	0.3714
404	69.85	40.19	1015.	148.3	0.3271	3600.	0.3208
405	69.46	39.31	1258.	168.9	0.2923	3600.	0.2865
406	69.76	39.85	1501.	186.3	0.2585	3600.	0.2531
407	69.95	40.29	2005.	221.2	0.2138	3600.	0.2091
408	69.95	40.04	2484.	248.1	0.1816	3600.	0.1773
Profile No. 1							
1101	70.05	9.32	249.7	44.8	0.5341	3300.	0.5038
1102	69.76	9.27	384.9	61.0	0.4678	3300.	0.4410
1103	70.05	10.78	506.5	74.8	0.4289	3300.	0.4039
1104	69.16	9.42	628.0	85.0	0.3935	3300.	0.3706
1105	69.85	9.61	753.0	98.2	0.3783	3300.	0.3563
1106	69.76	9.52	866.2	105.8	0.3522	3300.	0.3316
1107	69.66	9.66	1013.	117.7	0.3330	3300.	0.3134
1108	69.66	9.91	1140.	124.6	0.3104	3300.	0.2919
1109	69.76	9.52	1261.	130.9	0.2944	3300.	0.2768
1110	69.56	9.08	1378.	134.7	0.2764	3300.	0.2599
1111	69.76	9.27	1506.	140.8	0.2628	3300.	0.2470
1112	69.66	9.42	1754.	151.0	0.2387	3300.	0.2241
1113	69.56	9.81	2008.	161.3	0.2190	3300.	0.2055
1114	69.76	9.76	2244.	168.0	0.2022	3300.	0.1895
1115	69.95	9.95	2471.	176.7	0.1910	3300.	0.1789
1401	69.85	40.19	249.6	51.6	0.5184	3300.	0.4835
1402	69.95	40.29	503.2	85.8	0.4040	3300.	0.3751
1403	69.85	39.94	750.8	113.3	0.3429	3300.	0.3174
1404	69.76	40.09	1015.	140.7	0.3035	3300.	0.2801
1405	69.76	40.09	1255.	158.9	0.2655	3300.	0.2441
1406	69.85	39.94	1505.	176.4	0.2365	3300.	0.2167
1407	70.25	39.59	2012.	207.8	0.1938	3300.	0.1764
1408	69.95	39.06	2477.	230.1	0.1626	3300.	0.1469
Profile No. 2							
2101	69.85	10.10	249.4	44.8	0.5324	3000.	0.4782
2102	69.85	10.10	384.7	63.2	0.4832	3000.	0.4336
2103	69.95	10.20	507.1	76.8	0.4426	3000.	0.3969
2104	69.76	10.00	624.2	87.8	0.4090	3000.	0.3666
2105	69.85	10.35	753.7	100.6	0.3852	3000.	0.3450
2106	69.76	9.76	864.9	107.3	0.3575	3000.	0.3200
2107	70.25	10.73	1017.	119.8	0.3348	3000.	0.2992
2108	70.25	10.49	1130.	126.0	0.3157	3000.	0.2820
2109	70.15	10.43	1259.	133.3	0.2975	3000.	0.2655
2110	69.95	9.95	1376.	137.9	0.2818	3000.	0.2515
2111	69.95	10.44	1504.	143.8	0.2656	3000.	0.2367
2112	69.76	9.03	1749.	152.0	0.2426	3000.	0.2164
2113	69.76	10.00	2006.	162.6	0.2208	3000.	0.1964
2114	69.56	9.32	2237.	168.4	0.2048	3000.	0.1821
2115	69.76	9.52	2485.	174.9	0.1888	3000.	0.1676

Table 1 (*Contd.*)

2401	70.25	40.08	249.8	53.4	0.5412	3500.	0.5288
2402	70.05	39.64	502.1	88.1	0.4218	3000.	0.3688
2403	69.56	39.90	750.1	116.6	0.3571	3000.	0.3103
2404	69.76	40.09	1016.	145.0	0.3167	3000.	0.2736
2405	69.76	40.34	1258.	164.9	0.2791	3000.	0.2396
2406	69.56	39.90	1504.	182.9	0.2501	3000.	0.2135
2407	70.05	39.64	2004.	212.3	0.2020	3000.	0.1700
2408	69.85	39.70	2478.	233.8	0.1651	3000.	0.1366

Profile No. 3

3101	69.95	10.44	250.7	45.3	0.5348	3500.	0.5225
3102	70.15	10.39	384.0	62.5	0.4782	3500.	0.4671
3103	69.95	9.71	507.9	75.3	0.4341	3500.	0.4240
3104	69.85	9.37	625.4	87.1	0.4071	3500.	0.3976
3105	69.76	9.52	750.4	98.4	0.3806	3500.	0.3716
3106	69.66	9.66	866.2	107.7	0.3585	3500.	0.3500
3107	69.85	9.37	1018.	118.2	0.3339	3500.	0.3260
3108	69.85	9.61	1143.	125.4	0.3128	3500.	0.3054
3109	69.56	9.57	1262.	131.9	0.2962	3500.	0.2891
3110	70.05	10.05	1379.	137.0	0.2787	3500.	0.2720
3111	69.95	9.95	1503.	142.0	0.2636	3500.	0.2572
3112	69.66	9.42	1754.	152.4	0.2412	3500.	0.2352
3113	69.56	9.81	2005.	163.5	0.2229	3500.	0.2174
3114	69.76	10.00	2246.	172.3	0.2071	3500.	0.2019
3115	69.95	9.95	2485.	178.6	0.1922	3500.	0.1873
3401	69.76	39.85	250.7	52.7	0.5301	3500.	0.5158
3402	69.76	39.60	501.2	86.0	0.4216	3500.	0.4097
3403	69.66	39.50	750.9	116.9	0.3592	3500.	0.3486
3404	69.66	39.75	1014.	143.2	0.3127	3500.	0.3031
3405	69.85	40.19	1255.	161.9	0.2731	3500.	0.2643
3406	69.76	39.85	1501.	178.5	0.2421	3500.	0.2340
3407	69.85	40.43	2005.	210.5	0.1964	3500.	0.1892
3408	69.76	39.85	2484.	235.5	0.1661	3500.	0.1596

Profile No. 4

4101	70.05	10.54	250.5	48.5	0.5747	3450.	0.5588
4102	70.05	10.05	385.0	65.9	0.5059	3450.	0.4919
4103	69.56	9.08	507.5	81.8	0.4768	3450.	0.4637
4104	69.76	9.76	625.4	94.6	0.4434	3450.	0.4310
4105	69.95	10.20	752.0	106.6	0.4121	3450.	0.4005
4106	69.95	10.44	867.5	116.3	0.3869	3450.	0.3759
4107	69.95	9.95	1015.	126.6	0.3591	3450.	0.3489
4108	70.15	10.88	1143.	135.0	0.3353	3450.	0.3257
4109	69.76	9.27	1259.	139.9	0.3181	3450.	0.3091
4110	69.76	9.76	1376.	147.5	0.3043	3450.	0.2956
4111	70.05	10.05	1504.	153.0	0.2864	3450.	0.2780
4112	69.66	9.91	1753.	163.8	0.2602	3450.	0.2525
4113	69.85	9.86	2007.	174.8	0.2406	3450.	0.2335
4114	69.85	8.64	2242.	182.2	0.2263	3450.	0.2196
4115	69.66	9.91	2475.	192.7	0.2110	3450.	0.2046
4401	69.76	40.09	250.6	55.3	0.5626	3450.	0.5446
4402	69.56	39.65	505.2	94.8	0.4597	3450.	0.4444
4403	70.15	40.97	751.7	125.4	0.3902	3450.	0.3765
4404	69.76	40.09	1018.	153.1	0.3411	3450.	0.3288
4405	69.76	40.34	1259.	173.2	0.2996	3450.	0.2884
4406	69.95	39.79	1510.	191.3	0.2671	3450.	0.2568
4407	69.66	40.00	2005.	225.0	0.2205	3450.	0.2114

Profile No. 5

5101	70.05	10.29	249.2	45.2	0.5376	3500.	0.5288
5102	69.66	9.91	384.5	60.0	0.4578	3500.	0.4502
5103	69.76	10.00	504.1	76.2	0.4422	3500.	0.4349
5104	69.76	9.27	623.5	88.9	0.4175	3500.	0.4106
5105	70.15	10.39	749.4	100.5	0.3877	3500.	0.3811
5106	69.66	9.66	864.0	111.0	0.3716	3500.	0.3654
5107	69.95	10.69	1013.	122.0	0.3428	3500.	0.3369
5108	69.66	10.15	1137.	128.8	0.3220	3500.	0.3165
5109	69.56	9.81	1263.	135.0	0.3028	3500.	0.2977
5110	69.76	9.76	1377.	140.6	0.2881	3500.	0.2832
5111	69.85	10.10	1504.	146.4	0.2722	3500.	0.2675
5112	69.85	10.10	1756.	156.3	0.2457	3500.	0.2414
5113	69.95	9.71	2007.	167.7	0.2300	3400.	0.2227
5114	70.05	10.29	2234.	172.8	0.2085	3150.	0.1915
5115	69.76	10.00	2480.	178.8	0.1925	3150.	0.1768

Table 1 (*Contd.*)

5401	69.95	40.29	250.0	52.2	0.5246	3550.	0.5178
5402	69.95	40.04	503.5	89.6	0.4280	3550.	0.4222
5403	69.95	39.79	749.9	119.0	0.3683	3550.	0.3631
5404	69.85	39.94	1015.	146.7	0.3228	3550.	0.3180
5405	70.05	40.63	1259.	168.1	0.2860	3550.	0.2816
5406	69.95	41.02	1503.	186.3	0.2544	3550.	0.2504
Profile No. 6							
6101	70.05	10.54	249.7	46.5	0.5521	3450.	0.5394
6102	69.76	9.27	384.2	64.8	0.4998	3450.	0.4884
6103	69.95	9.95	507.4	79.5	0.4601	3450.	0.4494
6104	69.95	10.20	622.5	93.3	0.4378	3450.	0.4277
6105	69.76	9.27	752.3	103.9	0.4035	3450.	0.3941
6106	69.95	10.69	866.3	114.2	0.3791	3450.	0.3701
6107	69.95	9.71	1015.	124.0	0.3517	3450.	0.3434
6108	70.05	10.54	1140.	132.3	0.3299	3450.	0.3220
6109	69.95	9.95	1257.	137.3	0.3104	3450.	0.3029
6110	69.66	9.91	1378.	143.8	0.2947	3450.	0.2876
6111	69.76	9.76	1500.	149.3	0.2801	3450.	0.2733
6112	70.35	11.07	1758.	161.0	0.2511	3450.	0.2448
6113	69.56	10.54	2005.	172.0	0.2338	3450.	0.2279
6114	69.85	10.10	2195.	177.7	0.2202	2950.	0.1929
6115	69.85	9.61	2482.	188.4	0.2060	3200.	0.1919
6401	69.95	39.79	250.1	54.2	0.5510	3450.	0.5363
6402	69.85	39.70	502.7	92.3	0.4468	3450.	0.4343
6403	70.05	40.14	750.6	122.3	0.3808	3450.	0.3697
6404	70.25	40.33	1017.	151.5	0.3361	3450.	0.3260
6405	69.76	39.60	1262.	170.8	0.2949	3450.	0.2857
Profile No. 7							
7101	69.95	10.44	250.2	43.8	0.5170	3500.	0.5043
7102	69.36	9.13	384.9	60.7	0.4654	3500.	0.4540
7103	70.15	10.39	506.5	73.6	0.4230	3500.	0.4125
7104	69.95	9.71	623.6	86.4	0.4036	3500.	0.3936
7105	69.76	9.52	751.7	97.5	0.3761	3500.	0.3667
7106	69.95	9.71	865.6	106.2	0.3538	3500.	0.3449
7107	69.26	9.28	1016.	116.0	0.3274	3500.	0.3192
7108	70.15	11.12	1138.	123.8	0.3048	3500.	0.2970
7109	69.46	9.71	1263.	128.4	0.2864	3500.	0.2791
7110	69.95	9.71	1379.	134.8	0.2747	3500.	0.2677
7111	69.76	9.52	1502.	139.7	0.2603	3500.	0.2536
7112	69.85	9.61	1751.	148.8	0.2346	3500.	0.2284
7113	69.95	11.66	2012.	159.5	0.2097	3500.	0.2040
7114	69.85	9.61	2244.	163.7	0.1967	3500.	0.1914
7115	69.85	9.61	2493.	170.8	0.1826	3500.	0.1777
7401	69.46	39.80	258.4	48.0	0.4525	3500.	0.4392
7402	69.76	39.60	502.2	87.0	0.4143	3500.	0.4018
7403	69.85	40.19	749.9	115.4	0.3515	3500.	0.3404
7404	69.95	40.29	1018.	141.2	0.3035	3500.	0.2935
7405	69.95	40.78	1264.	161.2	0.2666	3500.	0.2573
7406	69.85	39.94	1504.	178.0	0.2401	3500.	0.2316
Profile No. 8							
8101	70.15	9.90	250.4	44.1	0.5223	3550.	0.5151
8102	69.95	10.20	385.6	64.5	0.4930	3550.	0.4862
8103	69.85	9.86	506.8	79.2	0.4589	3550.	0.4524
8104	69.95	9.47	629.8	91.1	0.4239	3550.	0.4180
8105	69.95	9.95	751.5	103.1	0.3986	3550.	0.3930
8106	70.15	10.39	865.7	111.9	0.3724	3550.	0.3670
8107	69.95	10.20	1017.	122.3	0.3443	3550.	0.3393
8108	69.85	10.10	1138.	127.3	0.3179	3550.	0.3133
8109	70.05	10.05	1261.	134.0	0.3007	3550.	0.2963
8110	69.95	10.20	1378.	138.2	0.2812	3550.	0.2770
8111	70.05	10.29	1506.	144.2	0.2665	3550.	0.2626
8112	70.15	10.88	1761.	152.1	0.2349	3550.	0.2314
8113	69.66	10.15	2011.	161.7	0.2182	3550.	0.2150
8114	70.05	10.29	2249.	166.7	0.1982	3550.	0.1951
8115	69.66	9.66	2490.	174.1	0.1868	3550.	0.1840
8401	70.05	40.63	251.0	51.8	0.5170	3550.	0.5085
8402	69.95	40.78	504.8	90.4	0.4293	3550.	0.4220
8403	69.85	39.94	752.2	119.9	0.3696	3550.	0.3631
8404	69.76	40.09	1017.	146.2	0.3200	3550.	0.3141
8405	70.25	39.84	1262.	166.4	0.2835	3550.	0.2781

Table 1 (*Contd.*)

8406	69.85	39.94	1506.	182.8	0.2497	3550.	0.2447
8407	69.95	39.79	2009.	215.0	0.2049	3550.	0.2005
8408	69.85	39.94	2496.	241.7	0.1721	3550.	0.1682
			Profile No. 9				
9102	69.66	9.42	385.1	64.5	0.4954	3600.	0.4882
9103	69.66	9.42	507.1	77.9	0.4515	3600.	0.4449
9104	69.36	8.64	625.4	92.2	0.4346	3600.	0.4283
9105	70.05	10.05	753.1	103.5	0.3991	3600.	0.3931
9106	69.76	9.76	865.5	113.5	0.3800	3600.	0.3743
9107	69.76	10.00	1016.	123.4	0.3483	3600.	0.3430
9108	69.95	9.95	1139.	131.2	0.3291	3600.	0.3241
9109	69.85	10.10	1266.	135.9	0.3037	3600.	0.2990
9110	69.95	10.20	1380.	141.8	0.2889	3600.	0.2845
9111	69.66	9.66	1503.	144.6	0.2697	3600.	0.2656
9112	69.16	8.69	1753.	154.7	0.2474	3600.	0.2436
9113	69.25	9.86	2009.	162.5	0.2208	3600.	0.2173
9114	70.05	10.05	2237.	168.5	0.2028	3600.	0.1995
9115	69.85	10.10	2496.	177.4	0.1891	3600.	0.1861
9401	70.05	40.63	250.3	51.4	0.5135	3600.	0.5046
9402	69.76	39.95	503.0	91.6	0.4418	3600.	0.4339
9403	69.95	40.04	751.6	121.2	0.3756	3600.	0.3686
9404	69.76	39.85	1019.	140.9	0.3314	3600.	0.3250
9405	70.05	40.38	1262.	169.3	0.2886	3600.	0.2828
9406	70.05	40.38	1507.	187.6	0.2581	3600.	0.2527
9407	69.66	40.00	2008.	219.0	0.2106	3600.	0.2058
9408	69.75	40.09	2466.	245.3	0.1775	3600.	0.1733

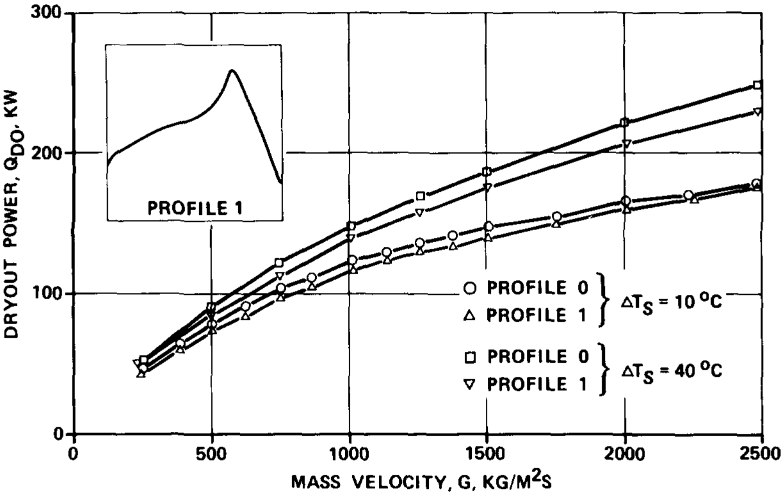

Figure 6. Measured dryout conditions.

stream section of the heated rod. For all of the test sections this segment was 150–400 mm long as shown in figures 4 and 5. The dryout locations for the different test sections and runs are found in table 1, where the given coordinate refers to the middle of the section where dryout was observed.

Four methods have previously been used for presenting experimental results for critical heat flux in channels with variable axial heat flux. Little (1970) and Becker (1969), for example, recommended the local hypothesis, while Lee & Obertelli (1963) used the total power hypothesis. Bertoletti *et al.* (1965) suggested the use of the boiling length hypothesis and Tong *et al.* (1965) developed the F-factor concept, which takes into account the details of the axial heat flux distribution. It is not the purpose of the present paper to discuss the mentioned hypothesis. This has been done elsewhere, e.g. Lahey & Moody (1975).

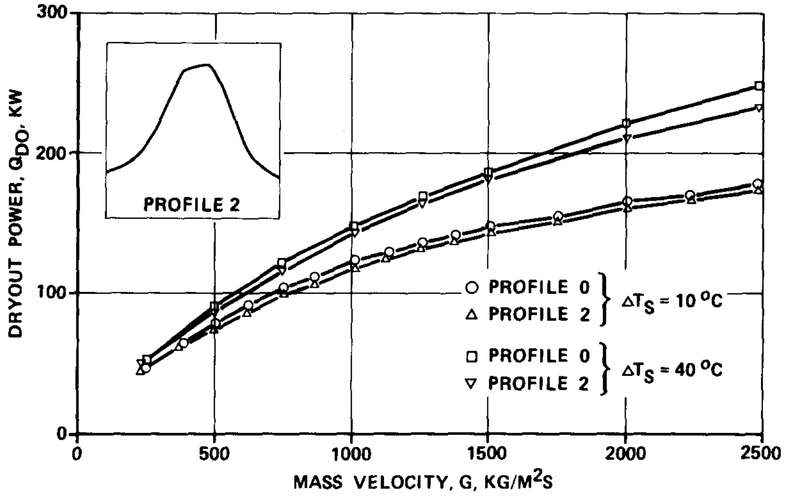

Figure 7. Measured dryout conditions.

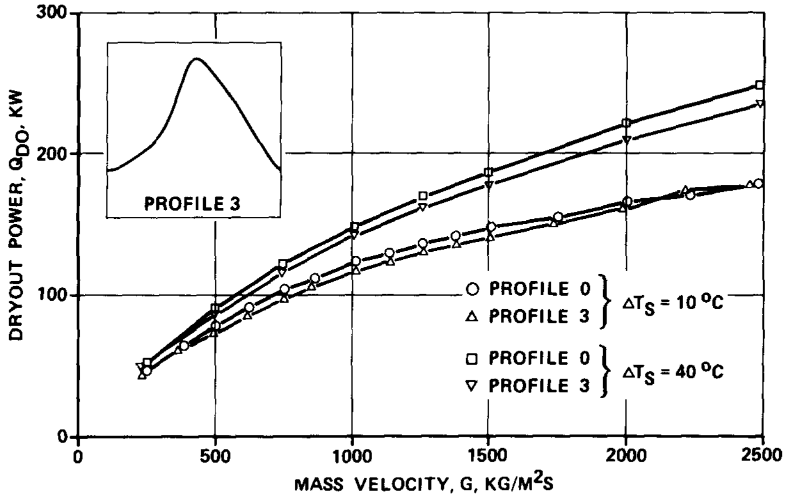

Figure 8. Measured dryout conditions.

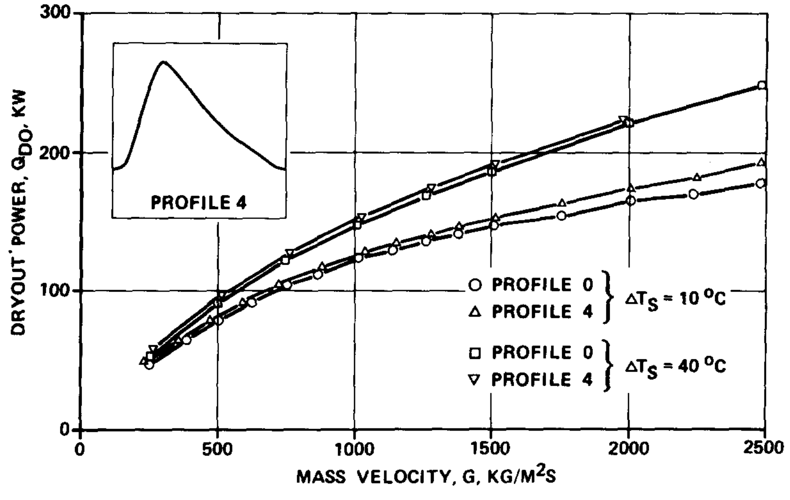

Figure 9. Measured dryout conditions.

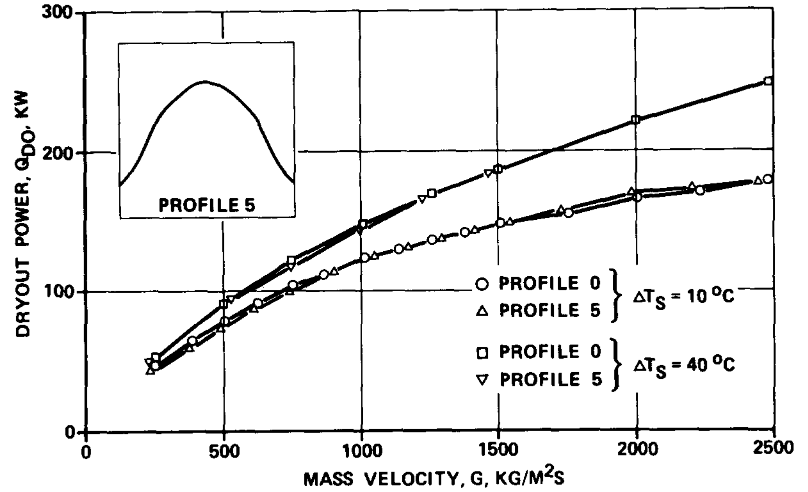

Figure 10. Measured dryout conditions.

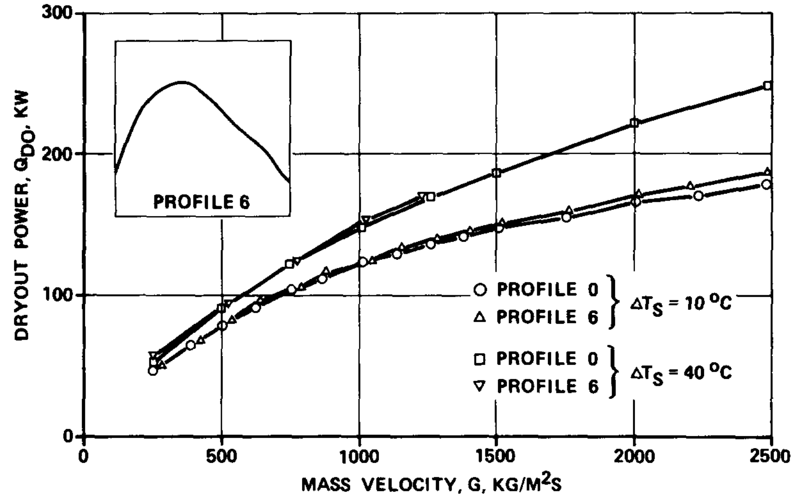

Figure 11. Measured dryout conditions.

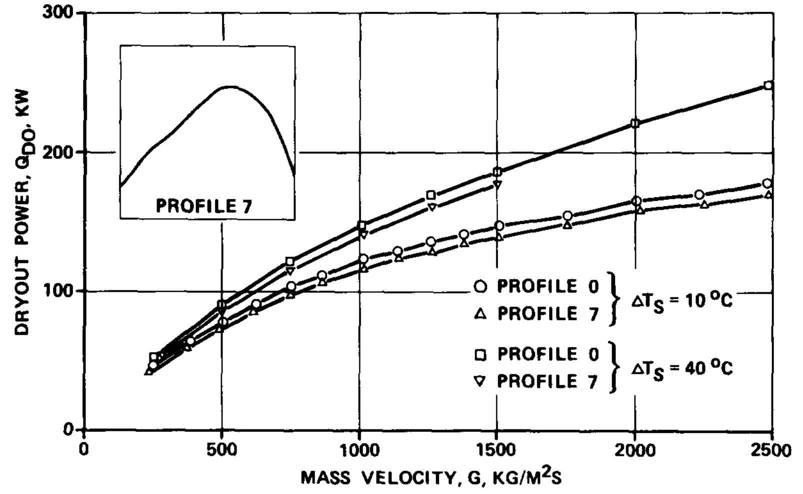

Figure 12. Measured dryout conditions.

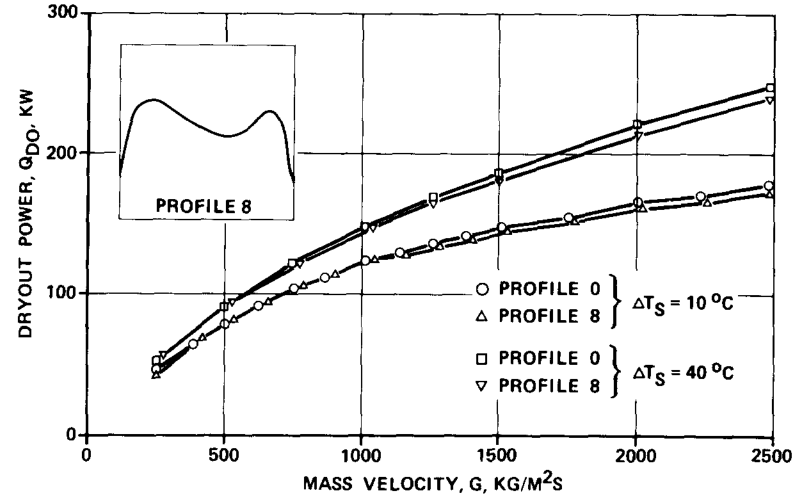

Figure 13. Measured dryout conditions.

Because the present experimental results appeared to be in satisfactory agreement with the total power hypothesis, this rather simple method was adopted for the following presentation of the data. Each of the figures 6–13 shows the experimental results for one axial profile in a plot of the total dryout power vs the mass velocity. To obtain a direct comparison with the uniformly heated test section, the diagrams also include the uniform heat flux results.

The experimental results for all the nine axial profiles are summarized in figure 14.

One observes that for the investigated annular geometry the effect of the axial heat flux distribution is relatively small. This result is supported by the 16-rod bundle measurements reported by General Electric (1973).

Except for a few runs at $G = 2250$ and $2500\ \mathrm{kg/m^2s}$ for profile 4, the effect of the flux profile upon the total dryout power is within ± 6 per cent of the results obtained for uniform heating. Although the deviations between the different flux profiles are rather small a few important observations will be mentioned.

The dryout power for the profiles 1, 2, 3, 5, 7, and 8 is in general low in comparison with the results for uniform heat flux, while the results for profiles 4 and 6 are high compared with uniform heat flux. The higher dryout power for profiles 4 and 6 is reasonable since these profiles have maximum heat flux in the upstream half of the annulus, while the other profiles have the

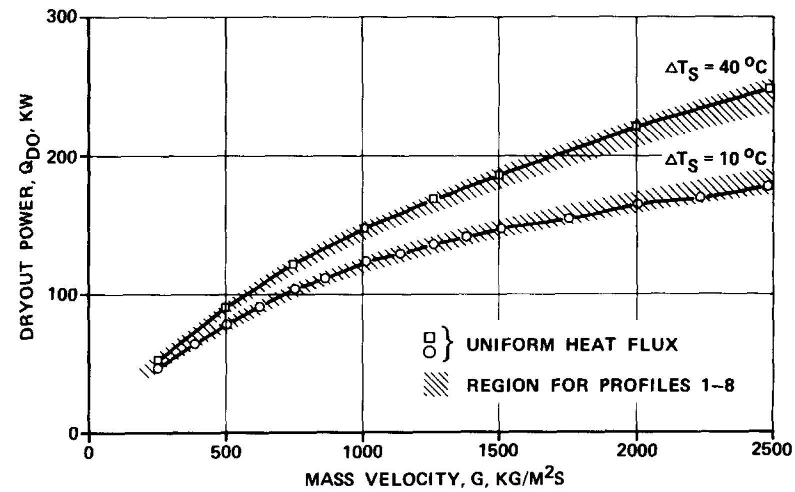

Figure 14. Summary of experimental results.

power peak in the downstream part of the test section or very close to the middle. Considering profile 8, which has two peaks, the data deviates only a few per cent from the uniform flux results.

Figure 15 shows a comparison between profile 1, which has a narrow downstream peak, and profile 4, which has a somewhat similar upstream peak. In the mass velocity range between 750 and 1500 kg/m^{2}s, which is of special interest for BWRs the difference in dryout power for the two cases is roughly 8 per cent.

A comparison of profile 6, which has a wide downstream peak and profile 7, which has a wide upstream peak, gives approximately the same difference in dryout power.

Differences in dryout power in the same range between inlet peaked and outlet peaked profiles are indicated by General Electric (1973) for 16-rod bundles, while round tube data by Judd *et al.* (1967) show significantly larger differences. It may be mentioned that the latter data were obtained with 72 in. tubes, which had axial peaking factors close to 2. This would perhaps explain the larger differences in dryout power.

Figure 16 shows a comparison between profile 1 with a narrow downstream peak and profile 7 with a wide downstream peak. The two profiles agree with one another within 2 per cent for mass velocities between 250 and 2000 kg/m^{2}s. Also the profiles 2, 3 and 5, which have approximately centered peaks but of different width, and profiles 4 and 6, that have a narrow respectively a wide upstream peak, indicate that the influence of peak width is small.

The dryout power for the uniform profile is significantly lower than for the upstream peaked profiles 4 and 6 and somewhat higher than the rest of the profiles. This is in contradiction to the 16-rod bundle tests by General Electric (1973), where the uniform profile had the highest dryout power of all the tested axial profiles, including one inlet peaked profile.

Lee & Bailey (1977) have compared 36-rod bundle data for uniform and chopped cosine axial profiles. At lower mass velocities there were no significant difference in the dryout power. For mass velocities above 2000 kg/m^{2}s, however, the cosine profile was about 6 per cent high. This result is in quite good agreement with our observations, provided profile 5 is considered to be equivalent to a cosine profile.

5. CONCLUSIONS

The most important result of the present investigation is the observation that for the present annular geometry the total dryout power is only to a relatively small extent affected by the axial heat flux profile.

However, a comparison with other investigations indicates that the effect of the axial profile

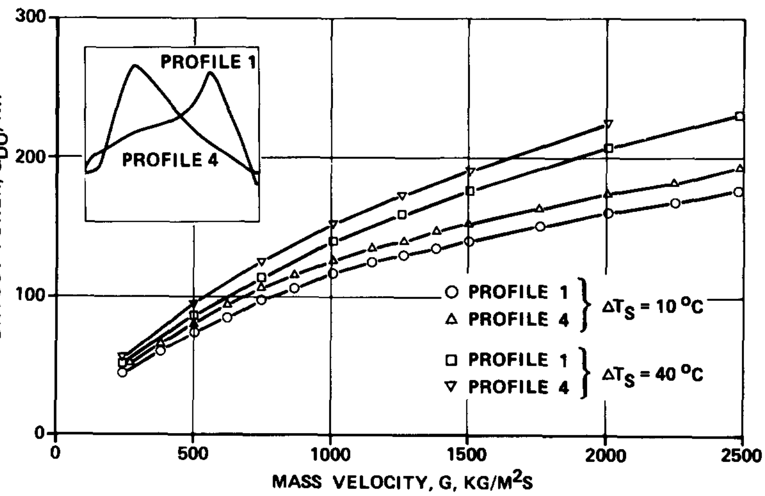

Figure 15. Measured dryout conditions.

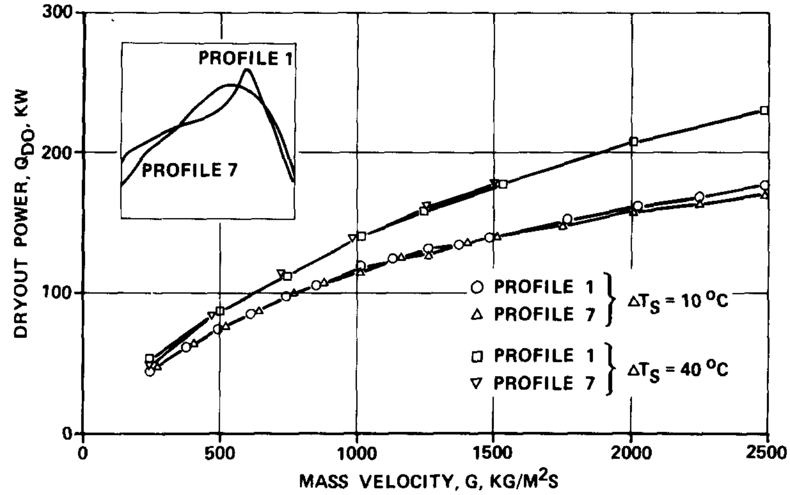

Figure 16. Measured dryout conditions.

is not unique. For rod bundles the situation is quite complex as cross-sectional geometry, spacer distance, spacer design and radial power distribution are parameters, which affect the influence on dryout of the axial heat flux distribution.

As known from rod bundle tests, dryout occurs predominantly just upstream of a spacer in the downstream part of the bundle. In the present tests the pin spacers obviously had negligible influence on the dryout location as with few exceptions dryout always occurred close to the downstream end of the rod. This fact may have contributed to the relatively small influence of the axial power profile. The conclusions obtained from the present study must therefore be applied with caution, when large rod bundles are considered.

Acknowledgements—The research reported in the present report was financed by ASEA-ATOM, Studsvik Energiteknik AB and the Swedish Board for Technical Development. Mr. G. Strand and Mr. S. Hedberg built the test section and participated in obtaining the experimental data. Their assistance is greatefully acknowledged.

REFERENCES

Becker, K. M., Hernborg, G., Bergman, K. & Lange, S. 1969 Measurements of Burnout conditions in vertical round tubes with non-uniform axial heat flux. AE-RL-1153.

Bertoletti, S. *et al.* 1965. Heat transfer crises with steam-water mixtures. *Energia Nucleare* **12**.

General Electric 1973 BWR thermal analysis basis (GETAB): data, correlation and design application. NEDO-10958, GEC.

Janssen, E. & Kervinen, J. A. 1963 Burnout conditions for non-uniformly heated rod in annular geometry, water at 1000 psia. GEAP-3755.

Judd, D. F., Wilson, R. H., Welch, C. P. & Lee, R. A. 1967 Non-uniform heat generation experimental program. Final Rep. Baw 3238–13.

Lahey, R. T. & C. Moody 1975 The thermal-hydraulics of a boiling water nuclear reactor. ANS Monograph.

Lahey, R. T. Gonzalez-Santalo, J. M. 1977 The effect of non-uniform axial heat flux on critical power. Paper C 219/7, *Heat and Fluid Flow in Water Reactor Safety Conf.* Manchester.

Lee, D. H. & Bailey, N. A. 1977 A review of experiments investigating the dryout characteristic of the SGHWR 36-Pin cluster. Paper E2, European Two-Phase Flow Group Meeting, Grenoble.

LEE, D. H. & OBERTELLI, J. D. 1963 An experimental investigation of forced convection burnout in high pressure water—II. Preliminary results for round tubes with non-uniform axial heat flux distribution. AEEW-R309.

LITTLE, R. B. 1970 Dryout tests on an internally heated annulus with variation of axial heat flux distribution. AEEW-R578.

TONG, L. S. 1972 Boiling Crisis and critical heat flux. TID-25887.

TONG, L. S. *et al.* 1965 Influence of axially non-uniform heat flux on DNB. WCAP-2767.